

Switching from Bonding to Nonbonding: Temperature-Dependent Metal Coordination in a Zinc(II) Sulfadiazine Complex

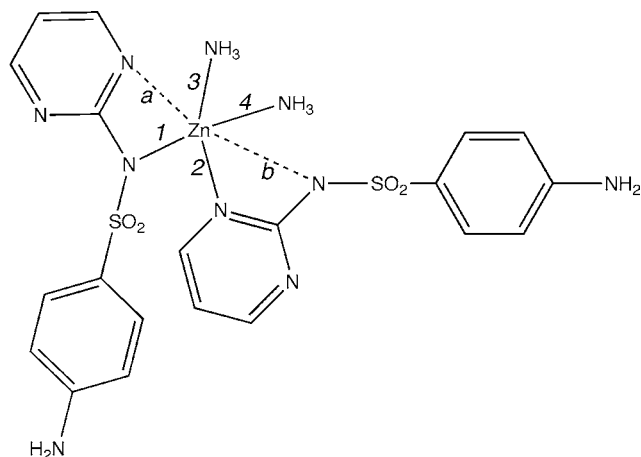
Fangfang Pan, Ruimin Wang, and Ulli Englert*

Institute of Inorganic Chemistry, RWTH Aachen University, 52056 Aachen, Germany

Supporting Information

ABSTRACT: The metal coordination in the mononuclear complex diamminebis(sulfadiazine)zinc shows a unique temperature dependence: High-resolution diffraction data prove that the coordination is almost tetrahedral at 100 K, whereas a fifth longer interaction becomes relevant at 200 K. The change in the geometry is fully reversible and is also reflected in the charge density of the compound.

The interactions between a metal center and its ligands represent the corner stone of coordination chemistry. These coordinative bonds create a plethora of structures and are decisive with respect to the reactivity of metal complexes in industrial and biological catalysis. The interatomic interactions in coordination compounds come in many different flavors: Their character can be predominantly covalent or ionic, and they may cover a wide range of distances. The second aspect is associated with an obvious problem in those popular cases in which structural and bonding information is retrieved from diffraction experiments. Their interpretation is mostly based on geometric considerations and may well be ambiguous: Should an interaction be considered a bond even if it is longer than expected? In this contribution, we will address the bonding situation in a zinc complex of the pharmaceutically active ligand sulfadiazine **1**. (Chart 1)

Chart 1. Scheme of Diamminebis(sulfadiazine)zinc(II) (**1**)^a

^aThe Zn–N interactions *a* and *b* drawn as dashed lines are significantly longer than the bonds 1–4.

Neither the compound nor the crystal structure is new: Two earlier reports^{1,2} agreed with respect to the outcome of single-crystal X-ray diffraction experiments at room temperature. We intended to shed light on the longer interactions labeled *a* and *b* in Chart 1 with the help of a charge density study.³ In order to deconvolute the deformation of the electron density due to bonding effects from thermal motion, high-resolution diffraction experiments at low temperature are mandatory. To our surprise, the metal coordination in **1** underwent clear-cut changes upon cooling that exceed the usual temperature effects by orders of magnitude. Temperature-dependent X-ray diffraction⁴ showed that the conformational change occurs between 100 and 200 K and is fully reversible; the basic features of molecular packing and the space group are preserved, and the changes in the conformation do not affect the crystal quality. At 200 K and at room temperature, the geometry corresponds closely to that described by the earlier authors. The relevant distances between the Zn^{II} cation and the surrounding N donors at all three temperatures have been compiled in Table 1.

Table 1. Coordination Geometry in Compound **1** at 100, 200, and 293 K^a

interaction	distance [Å]		
	100 K	200 K	293 K
1	2.0573(5)	2.143(3)	2.165(3)
2	2.0646(5)	2.071(3)	2.075(3)
3	2.0238(5)	2.029(3)	2.032(4)
4	2.0433(5)	2.049(3)	2.038(3)
<i>a</i>	2.7009(5)	2.428(3)	2.400(3)
<i>b</i>	2.8382(4)	2.750(3)	2.719(3)

^aInteraction labels have been assigned in Chart 1.

Table 1 shows that the most significant changes occur between 100 and 200 K. The results from our own diffraction experiment at room temperature have been included for comparison and confirm that a further increase in the temperature does not have a major influence on the molecular structure. The effect observed between 100 and 200 K is very pronounced for the presumably weaker interactions *a* and *b*, with both being much shorter at the higher temperature. The four shortest interactions, 1–4, are unexceptional; at 100 K, they fall into the range of conventional Zn–N coordination bonds. In contrast to the secondary interactions *a* and *b*, these

Received: October 24, 2011

Published: December 22, 2011

unambiguous bonds are longer in the case of the 200 K conformer; the maximum effect is observed for *1*. A comparison with the Cambridge Structural Database⁵ supports the idea that the 200 K structure is on the way to pentacoordination: For 261 crystal structures⁶ featuring a tetracoordinated Zn center bonded to four N atoms, the average Zn–N distance amounts to 2.015 Å, with 1.978 Å for the lower quartile and 2.051 Å for the upper quartile. Interaction *1* in the 200 K conformer clearly exceeds this value. In addition to variation in the bond distances, several angles subtended by *1*–*4* at the central cation change, too: At 100 K, these angles are close to tetrahedral, with values between 100.47(2) and 122.04(2)°, whereas the coordination is more distorted at 200 K, with angles ranging from 94.44(11) to 134.32(13)°. The conformer associated with the higher temperature adopts a less symmetric coordination because of the steric requirements of the approaching additional bonding partner, a pyrimidine N atom. This change in the geometry can be perceived in Figure 1, a superposition of the molecular conformations at 100 and 200 K.

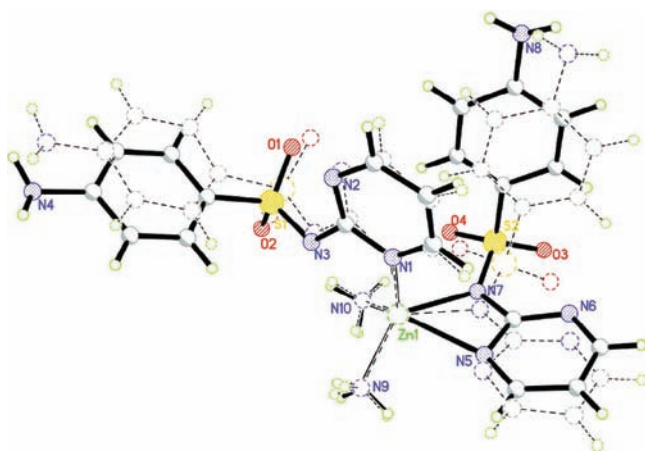


Figure 1. Superposition plot (*SHELXTL* 2008/1,⁷) of the molecular structures of **1** at 100 K (dashed) and 200 K (solid).

Along with this change in the coordination geometry, one of the ammine ligands rotates around the Zn–N bond. Although the qualitative packing characteristics are maintained at higher temperatures, several intermolecular hydrogen bonds undergo small but significant changes. A detailed overview about the molecular geometries and hydrogen bonds at both temperatures is provided in the Supporting Information. The temperature-dependent diffraction experiments also showed that, contrary to common experience, the unit cell of **1** does not simply expand upon heating: We rather observe a maximum for the cell volume around 150 K, with values of 2469.7(2) Å³ at 100 K and 2465.8(13) Å³ at 200 K, a fact that also indicates a major change in the molecular structure: For both the low- and high-temperature conformers, the unit cell will most likely expand in a rather smooth fashion; if this expansion is more pronounced for the 100 K geometry, a local maximum for the cell volume may be encountered. A figure showing the unit cell volume as a function of the temperature is available in the Supporting Information. Fortunately, insight into chemical bonding is not necessarily limited to the purely geometric arguments discussed above but can also be based on the electron density. This quantity may, in principle, be obtained either from high-resolution X-ray diffraction experiments or from theoretical calculations. In the case of **1**, excellent crystals

were available; therefore, a low-temperature diffraction experiment followed by multipole refinement^{8,9} resulted in an experimental charge density for the structure at 100 K. In view of the fact that thermal motion prevents an experimental charge density study at higher temperatures, we recurred to the well-characterized situation at 100 K as the test case for an alternative theory-based access to the electron density: A single-point calculation based on the so-called independent atom model, the conventional structure model for the 100 K data, afforded a theoretical electron density;¹⁰ from this electron density, structure factors were generated¹¹ and treated in the same way as the experimental data. Both densities, that based entirely on the experiment and the alternative derived from theoretical structure factors, were analyzed in terms of Bader's Atoms In Molecules (AIM) theory.¹² For the geometry derived from the 100 K data, both densities had very similar topological properties with respect to the position, the electron density, and the Laplacian of all bond critical points associated with covalent bonds within the ligands and coordinative bonds between the ligands and the metal. For interactions in the zinc coordination sphere, a comparison is provided in the Supporting Information. This good match between direct experimental and theoretically derived electron densities at lower temperature confirmed that the theoretical approach represents a valid alternative and that the same procedure may also be used for analysis of the 200 K conformer. In Figure 2, plots of the electron density gradients allow one to compare the bonding situation at both temperatures.

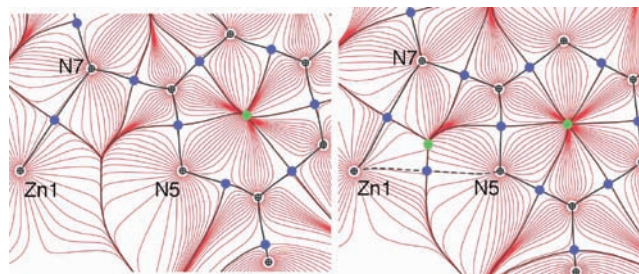


Figure 2. Gradient vector field of the electron densities at 100 K (left) and 200 K (right). Bond paths are shown as black lines, bond critical points as dark-blue solid circles, and ring critical points as green solid circles. Topological properties of the interaction Zn1–N5 at 200 K: $\rho = 0.223 \text{ e } \text{Å}^{-3}$; $\nabla^2\rho = 2.62 \text{ e } \text{Å}^{-5}$.

The most obvious difference between the coordination geometry of **1** at 100 K (Figure 2, left) and that at 200 K (Figure 2, right) resides in the presence of a bond critical point in the latter: The interatomic distance Zn–N5, denoted as *a* in Chart 1, is not just significantly shorter at higher temperature but can also be assigned a bond path. This feature of the electron density indicates a bonding interaction¹³ but not necessarily a conventional chemical bond.^{14,15} In particular with respect to very weak contacts, it has been debated whether the mere existence of a critical point can be considered sufficient for identifying a specific interaction as a bond.¹⁶ In the present case, however, the electron density in the bond critical point for the longer fifth interaction *a* indicates appreciable and chemically relevant bonding: It amounts to $0.223 \text{ e } \text{Å}^{-3}$, a value almost as high as that found for Zn–N bonds in octahedral complexes¹⁷ and comparable with moderately strong hydrogen bonds.¹⁸ The Laplacian of the electron density corroborates this interpretation: Figure 3 shows the temper-

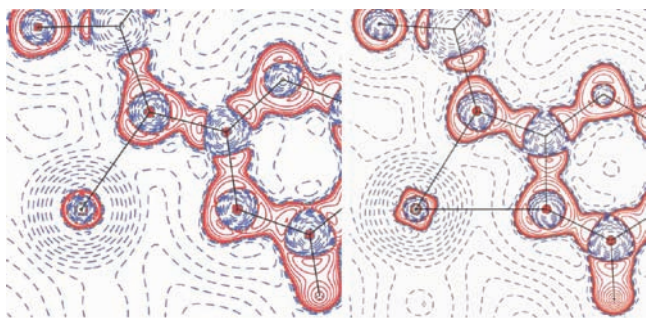


Figure 3. Laplacian of the electron densities at 100 K (left) and 200 K (right). Positive values are in blue and negative values in red; contours are at $\pm 2n \times 10^{-3} \text{ e } \text{Å}^{-5}$ ($0 \leq n \leq 20$).

ature dependence of polarization for the pyrimidine N atom; at higher temperature (right), its lone pair is oriented more toward the direction of the cation.

Interactions between (often, but not necessarily cationic) metal centers and their donor atoms can in many cases be associated with the ionic character, and these electrostatic interactions are more distance-tolerant than orbital-overlap-dominated covalent bonds. In this contribution, we have presented a rare example for a complex with temperature-dependent coordination: Our experimental data have shown unambiguously that the increase in the temperature is sufficient to trigger a reversible conformational change, during which a new balance between molecular coordination and intermolecular interactions is established. Our example provides an additional reason not to overinterpret the results from conventional X-ray diffraction experiments!

■ ASSOCIATED CONTENT

📄 Supporting Information

Analytical data for **1**, description of the methods in diffraction experiments and theoretical calculations, plot of the scale factor distribution and summary of completeness for the experimental charge density data, detailed tables with crystal data, data collection parameters, and convergence results for the independent atom model at 100 and 200 K and for the multipole model at 100 K, displacement ellipsoid plots at 100 and 200 K, table with relevant interatomic distances and angles at 100 and 200 K, table with donor–acceptor distances in hydrogen bonds at 100 and 200 K, table with the topological properties for all bond critical points, comparison between the topological properties of the experimental and theoretical charge densities at 100 K and the theoretical density at 200 K for bonds involving the metal cation, figure showing the unit cell volume as a function of the temperature, powder diffractograms at 100 and 200 K, and crystallographic information for diffraction experiments at 100, 200, and 293 K in CIF format. This material is available free of charge via the Internet at <http://pubs.acs.org>.

■ AUTHOR INFORMATION

Corresponding Author

*E-mail: ullrich.englert@ac.rwth-aachen.de.

■ ACKNOWLEDGMENTS

This work has been funded by a fellowship to F.P. from the China Scholarship Council and by DFG (Priority Program 1178, *Experimental Charge Density as the Key to Understand*

Chemical Interactions). We thank Thomas Dols for collecting high-resolution X-ray data and Birger Dittrich for helpful discussions.

■ REFERENCES

- (1) Baenziger, N. C.; Modak, S. L.; Fox, C. L. Jr. *Acta Crystallogr., Sect. C* **1983**, *39*, 1620–1623.
- (2) Brown, C. J.; Cook, D. S.; Sengier, L. *Acta Crystallogr., Sect. C* **1985**, *41*, 718–720.
- (3) Coppens, P. *X-ray Charge Densities and Chemical Bonding*; Oxford University Press: Oxford, U.K., 1997.
- (4) Crystal data for **1**: $\text{C}_{20}\text{H}_{24}\text{N}_{10}\text{O}_4\text{S}_2\text{Zn}$, $M = 597.98$, orthorhombic, space group $Pna2_1$ (No. 33). At 100 K: $a = 13.6653(6) \text{ Å}$, $b = 12.8420(6) \text{ Å}$, $c = 14.0734(7) \text{ Å}$, $V = 2469.7(2) \text{ Å}^3$, $Z = 4$, $D_c = 1.607 \text{ g cm}^{-3}$, $\mu = 1.213 \text{ mm}^{-1}$, 26 417 reflections measured, 6777 unique ($R_{\text{int}} = 0.0372$). Final wR2 (all data) = 0.0785, and final RI = 0.0304. At 200 K: $a = 13.800(4) \text{ Å}$, $b = 12.646(4) \text{ Å}$, $c = 14.130(4) \text{ Å}$, $V = 2465.8(13) \text{ Å}^3$, $Z = 4$, $D_c = 1.607 \text{ g cm}^{-3}$, $\mu = 1.216 \text{ mm}^{-1}$, 21 243 reflections measured, 4963 unique ($R_{\text{int}} = 0.0545$). Final wR2 (all data) = 0.0821, and final RI = 0.0344. Further details on the multipole refinement of the 100 K data are given in the Supporting Information.
- (5) Allen, F. *Acta Crystallogr., Sect. B* **2002**, *58*, 380–388.
- (6) Database version of Nov 2010, 525095 entries, error-free structures with $T < 200 \text{ K}$ only.
- (7) Sheldrick, G. M. *SHELXTL 2008/1, Structure Determination Software Suite*; Bruker AXS: Madison, WI, 2008.
- (8) Hansen, N. K.; Coppens, P. *Acta Crystallogr., Sect. A* **1978**, *34*, 909–921.
- (9) Volkov, A.; Macchi, P.; Farrugia, L. J.; Gatti, C.; Mallinson, P. R.; Richter, T.; Koritsanszky, T. *XD2006*; University of New York at Buffalo, Buffalo, NY, 2006.
- (10) Frisch, M. J. et al. *Gaussian 03*, revision E.01; Gaussian, Inc.: Wallingford, CT, 2004.
- (11) Jayatilaka, D.; Grimwood, D. J. *Comput. Sci. ICCS* **2003**, *2660*, 142–151.
- (12) Bader, R. F. W. *Atoms in Molecules—a Quantum Theory*; Clarendon Press: Oxford, U.K., 1990.
- (13) Bader, R. F. W. *J. Phys. Chem. A* **1998**, *102*, 7314–7323.
- (14) Bader, R. F. W. *J. Phys. Chem. A* **2009**, *113*, 10391–10396.
- (15) Stalke, D. *Chem.—Eur. J.* **2011**, *17*, 9264–9278.
- (16) Dunitz, J. D.; Gavezzotti, A. *Angew. Chem., Int. Ed.* **2005**, *44*, 1766–1787.
- (17) Wang, R.; Lehmann, C. W.; Englert, U. *Acta Crystallogr., Sect. B* **2009**, *65*, 600–611.
- (18) Šerb, M.; Wang, R.; Meven, M.; Englert, U. *Acta Crystallogr., Sect. B* **2011**, *67*, 552–559.